Journal of Materials Chemistry C

ROYAL SOCIETY OF CHEMISTRY

PAPER

View Article Online
View Journal | View Issue

Cite this: J. Mater. Chem. C, 2021, 9, 10317

Retention of perylene diimide optical properties in solid-state materials through tethering to nanodiamonds†

Asia R. Y. Almuhana,[a] Philipp Langer,[b] Sarah L. Griffin,[a] Rhys W. Lodge,[b] Graham A. Rance [bc] and Neil R. Champness *[a]

Received 4th June 2021,
Accepted 23rd July 2021

DOI: 10.1039/d1tc02577e

rsc.li/materials-c

The synthesis of nanodiamond-perylene diimide composites is reported. Suitably hydroxyl-functionalised perylene diimides (PDIs) are reacted with carboxylic acid functionalised nanodiamonds (NDs) through ester formation. The ND-PDI nanocomposite materials were characterised using a variety of different techniques confirming retention of the ND cores and interestingly the dye properties of the PDIs. In particular, fluorescence measurements suggest that PDIs tethered to NDs retain the characteristics of solution-phase PDIs rather than the optical properties associated with solid-state PDIs which are typically modified due to aggregation. Our relatively simple approach provides a mechanism for maintaining the solution-phase properties of PDIs in solid-state materials.

Introduction

Perylene diimides (PDIs) are a class of polyaromatic dye molecules which have widespread use across many fields that employ their strong absorbance, fluorescence and *n*-type semiconducting properties.[1,2] In combination with their excellent photochemical and thermal stabilities,[1–4] PDIs have found applications in a variety of organic electronic devices, including field effect transistors,[5–7] light emitting diodes,[8–10] and photovoltaic cells.[11–13] One of the most attractive features of PDIs is that their properties can be tuned through suitable functionalisation, either of the aromatic core or through thionation of the carbonyl groups. Notably, chemical functionalisation of the imide nitrogen with carbon-based groups, *e.g.* alkyl or aryl groups, barely influences the properties of the core and thus provides a simple method of attaching the PDI to larger species, for example polymers[14,15] or nanoparticles,[16,17] whilst retaining the PDI's most interesting physicochemical features.

The properties of PDIs are significantly affected by aggregation,[2,18] and thus it is common that in the solid-state PDIs exhibit different properties to those that are observed in solution.[19] In particular, aggregation of PDIs typically leads to changes in the UV-visible absorption profile, notably as a result of H-aggregation,[20,21] and fluorescence quenching is a common feature of solid-state PDI aggregates.[22] Some notable examples of PDIs that preserve attractive solution-phase optical properties in the solid-state are known, but typically require the introduction of sterically-inhibiting groups that prohibit stacking of the PDI aromatic cores.[23–34] In this study, we use a different approach of anchoring PDIs to the surface of nanodiamonds (NDs) in order to inhibit stacking between adjacent dye molecules and by so-doing we are able to retain the solution-phase PDI properties, specifically fluorescence, in solid-state materials.

NDs represent a valuable member of the diverse family of nanocarbons – a group which also includes nanoscale amorphous carbon, fullerenes, diamondoids (NDs with a size of 1–2 nm), nanotubes, onions, diamond rods and foams.[35–37] NDs were first synthesised by detonation and studied in Russia in the 1960s; however, they did not become of wide interest to the scientific community until the 1980s.[38,39] Significant research in the area has subsequently developed due to the unique structural, chemical, optical, and biological characteristics[35] and excellent photostability of NDs.[40] Attractive mechanical properties enable their use in films for robust implant coatings[41] and as additives in lubricants.[42] The structure of NDs comprises a core of sp^3-hybridised carbon atoms, which is diamond-like in character, coated with a semi graphitic sp^2-hybridised carbon shell.[43] Thus, as the chemistry of related graphitic systems, *e.g.* carbon nanotubes, is well known,[44] these approaches can in principle be adapted for the surface functionalisation of NDs. Moreover, upon

[a] School of Chemistry, University of Birmingham, Edgbaston, Birmingham, B15 2TT, UK. E-mail: n.champness@bham.ac.uk
[b] School of Chemistry, University of Nottingham, University Park, Nottingham, NG7 2RD, UK
[c] Nanoscale and Microscale Research Centre (nmRC), University of Nottingham, University Park, Nottingham, NG7 2RD, UK

† Electronic supplementary information (ESI) available. CCDC 2085715. For ESI and crystallographic data in CIF or other electronic format see DOI: 10.1039/d1tc02577e

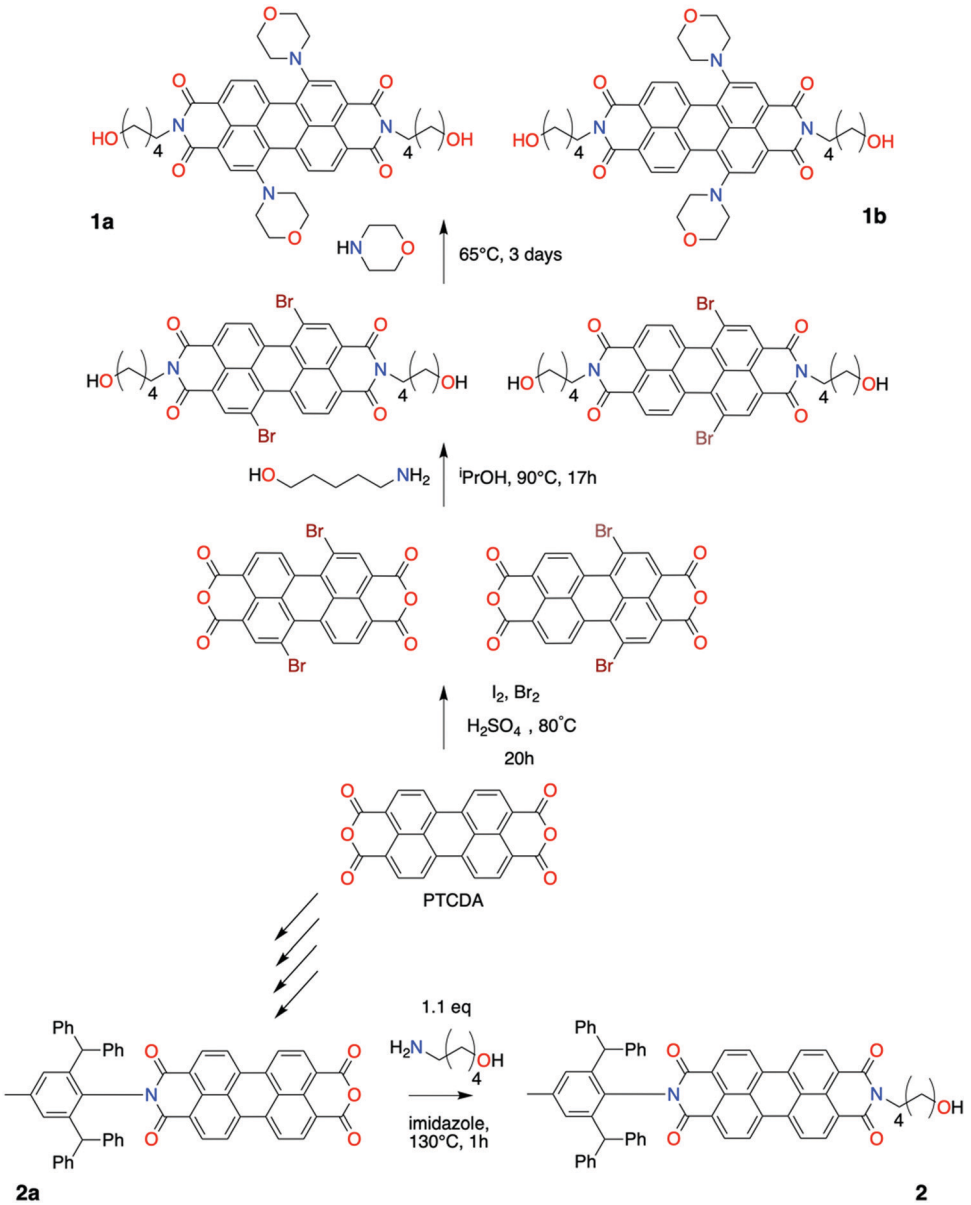

Scheme 1 Synthetic paths to hydroxyl functionalised PDIs **1a**, **1b** and **2**.

functionalisation the diamond core remains intact allowing chemical reactions to be performed at their surfaces without disrupting the inherent interior structure of the diamond-like nanoparticle. A range of chemical, wet and gas techniques have been used to modify ND surfaces in order to tailor their properties, with the resulting composites finding broad-ranging applications, such as in polymer coatings[45] and grafts.[46–48] Herein, we employ the functionalisation of the surface of NDs by a facile oxidative process, introducing carboxylic acid groups, to allow subsequent reactions with suitably functionalised PDIs. Our approach allows functionalisation of the surface of NDs and retention of the optical properties of PDIs whilst anchored to the solid ND particles.

Results and discussion

To functionalise the exterior surface of NDs with PDIs we reacted carboxylated NDs with PDIs with pendent hydroxyl groups, forming ester links between the NDs and PDIs. Our strategy required three main steps: (i) synthesis of suitably functionalised PDIs; (ii) oxidation of NDs to form carboxylic acid groups on their surface; and (iii) esterification of the oxidised ND with the hydroxyl-functionalised perylene diimide.

Three different PDIs with hydroxyl groups pendent to the imide groups were synthesised, designated **1a**, **1b** and **2** (Scheme 1). A key synthetic issue when using PDIs is their tendency to aggregate, typically leading to low solubility,[2,18] and therefore strategies to improve solubility have been developed.[2]

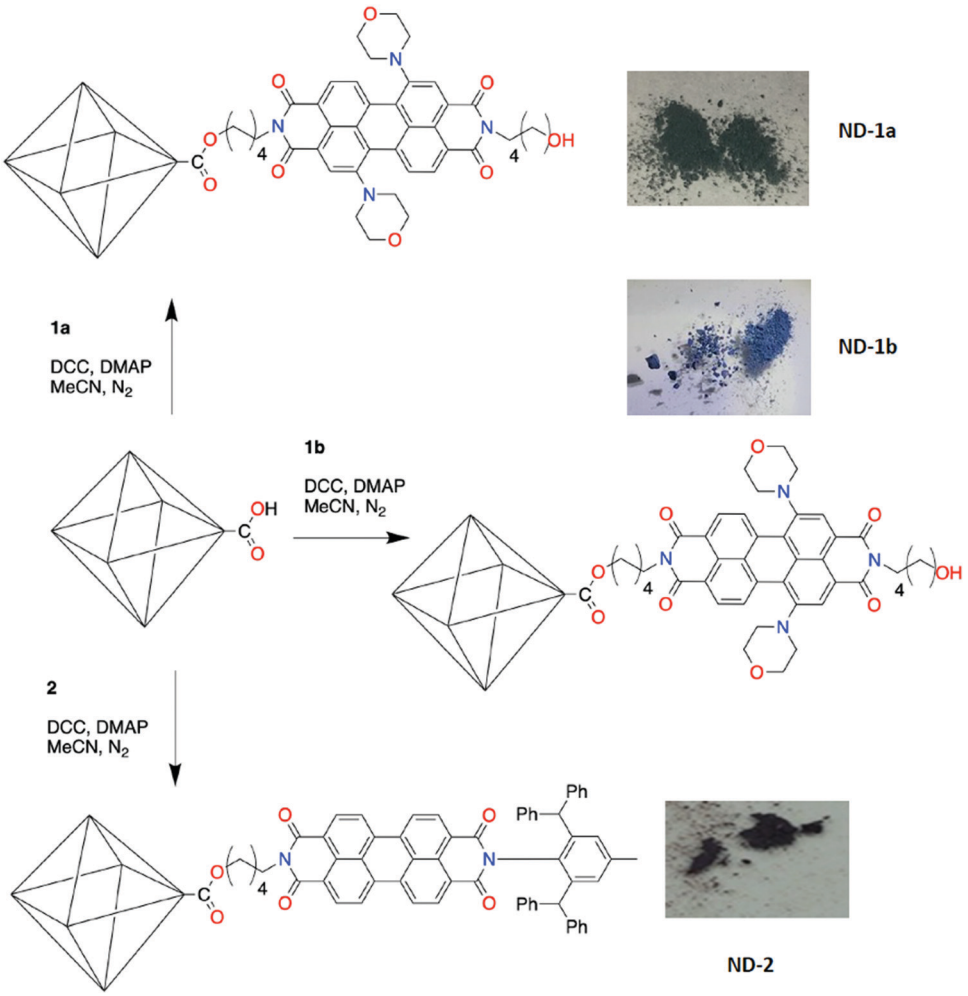

Fig. 1 Preparation conditions for PDI-functionalised NDs and photographs showing the subsequent powdered samples.

In this study, we have taken two approaches: firstly, the introduction of substituents into the bay region of the PDI, in this case two morpholine groups, as either the 1,7 (**1a**) or 1, 6 (**1b**) isomer. The central 1, 6, 7 and 12 positions of PDIs are colloquially known as the 'bay region', presumably due to the resemblance of this component of the aromatic scaffold to a coastal 'bay'. Bay-substitution reduces stacking, although dimeric arrangements are observed in the solid-state, and also infer distinct optical and redox properties on the PDI as a result of the tertiary amine substituents in comparison to other PDIs.[49–51] A stepwise synthetic approach was taken introducing the pendent pentyl hydroxyl groups to dibromo-perylene dianhydride[52] *via* reaction with 5-aminopentanol, then subsequent substitution of the bromide through reaction with morpholine. This pathway afforded the two isomers, 1,7 (**1a**) and 1,6 (**1b**) substituted, which were separated by column chromatography, and successfully lead to PDI species with pendent hydroxyl groups that can be subsequently used for the esterification step. The single crystal X-ray diffraction structure of **1a** illustrated that the molecules are stacked in pairs in the solid-state (Fig. S1, ESI†). This arrangement is common with 1, 7-disubstituted PDI molecules,[49–51] where the bay-region substituents restrict access to one face of the perylene core allowing stacking with only one other adjacent PDI. The hydroxyl groups are involved in hydrogen bonds with hydroxyl groups from adjacent molecules (O···O = 2.65 Å).

In our second approach, different functional groups were introduced to the imide positions. To achieve this desymmetrisation, we prepared the monoamide–monoanhydride **2a** following our previously reported approach.[53] Compound **2a** was then reacted with 5-aminopentanol to afford **2**. Although the 2, 6-(bis)diphenylmethyl-4-methylphenyl group used to occupy one of the imide termini is sterically inhibiting, such asymmetrically functionalised PDIs still aggregate in the solid-state through stacking of the exposed portion of the PDI.[53] The targeted ND-PDI nanocomposites, **ND-1a**, **ND-1b** or **ND-2**, were synthesised using a Steglich esterification, reacting nanodiamonds possessing surface-based carboxylic acid groups, **ND-COOH** (following oxidation of the as-received **ND** using literature protocols),[54] with the corresponding PDI (**1a**, **1b** or **2**). The dispersed phase remained stably suspended in acetonitrile after stirring for 48 h at room temperature under a dinitrogen atmosphere, with the solid product isolated and purified using consecutive cycles of centrifugation and washing with acetonitrile, ethanol and chloroform,

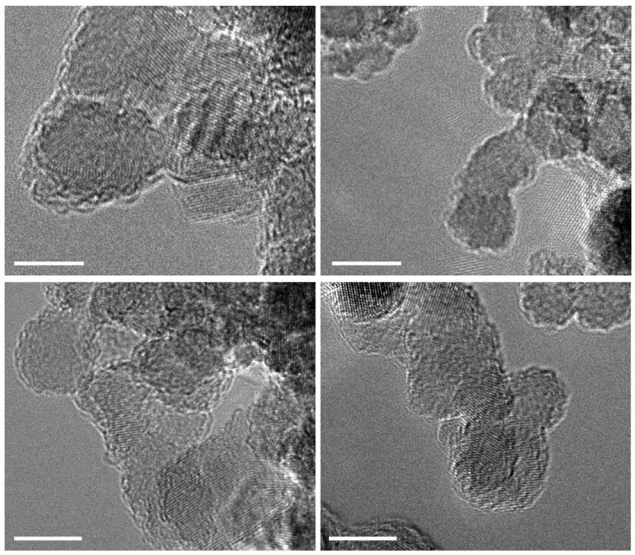

Fig. 2 TEM imaging of (a) **ND-COOH**, (b) **ND-1a**, (c) **ND-1b**, and (d) **ND-2**. A d-spacing of 0.207 nm is consistent with the (111) plane of cubic diamond. Scale bars are 5 nm.

and finally drying in an oven at 50 °C for 24 h. The resulting powders inherit the colours of the parent PDI dye: **ND-1a** is green, **ND-1b** has a light blue colour and **ND-2** is red (Fig. 1).

A variety of techniques were employed to study the effect of PDI-functionalisation on the NDs. Whilst Raman spectroscopy (Fig. S2, ESI†) was successfully used to confirm the retention of the diamond core and introduction of surface carboxylic acid groups in **ND-COOH**, following oxidation of **ND** in a mixture of HNO_3 and H_2SO_4,[55] strong fluorescence from the PDIs in the ND-PDI samples negated its use thereafter (Fig. 3). However, IR spectra of the ND-PDI systems (Fig. S3, ESI†) showed a new peak at 1732 cm^{-1}, attributed to the stretching vibration of the ester C═O, accompanied by a significant increase in the intensity of peaks at 2919 and 2950 cm^{-1} which arise from C–H stretching vibrations.[56] Both changes were consistent with the PDI species being chemically attached to the ND surfaces. Thermogravimetric measurements support the covalent nature of the grafting (Fig. S4, ESI†), with the thermal stability of the ester bond unusually high, up to ~550 °C in air, compared to literature results (~300 °C in air).[55] This is especially noteworthy as the pure perylene was found to decompose at a similar temperature of ~550 °C in air.

Transmission electron microscopy (TEM) confirmed the expected structure of nanodiamonds: a ~5 nm crystalline diamond-like core surrounded by a more disordered, semi-graphitic shell (Fig. 2). Functionalisation of NDs with PDIs seemingly induces no significant change in the surface structure of individual nanodiamonds or their extent of aggregation; however, energy dispersive X-ray (EDX) spectroscopy (Fig. S5, ESI†) confirmed the success of this synthetic step, with an increase in the oxygen content in the ND-PDIs (1.1, 1.7 and 1.8% for **ND-1a**, **ND-1b** and **ND-2**, respectively), relative to the parent **ND-COOH** (~1.0%), consistent with the additional oxygen atoms in the PDI species. It is important to note that

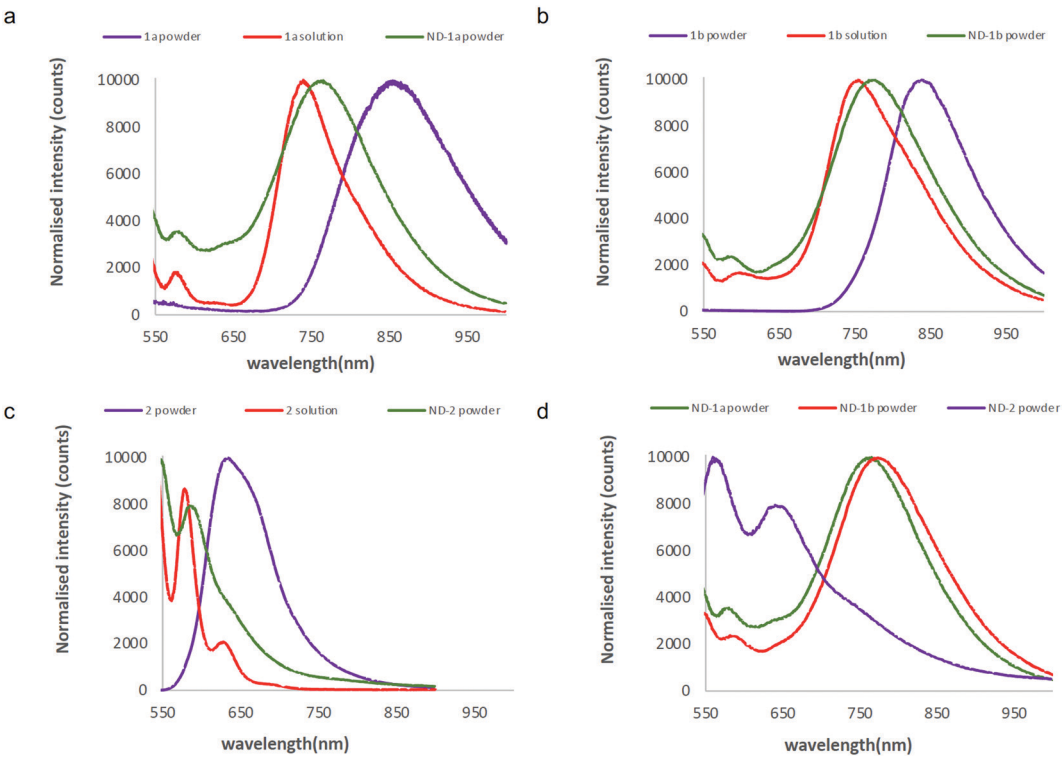

Fig. 3 Normalised fluorescence spectra comparing the different ND-PDIs (green), parent PDI in solid-state (purple) and in chloroform solution (red). (a) **ND-1a**/**1a**; (b) **ND-1b**/**1b**; and (c) **ND-2**/**2**. (d) Comparison of spectra for **ND-1a** (green), **ND-1b** (blue), **ND-2** (purple).

EDX spectra were captured from small clumps of nanoparticles hanging over a hole in the support film to avoid signal from the support film itself. No nitrogen was detected in the EDX spectra of the ND-PDIs, indicating the extent of PDI grafting is below the threshold sensitivity for the detector.

Nanodiamonds are widely known to aggregate in suspension – the aggregates observed in TEM images likely reflect an artefact of the drying procedure used for TEM specimen preparation – and so to probe this more directly samples were dispersed in chloroform and analysed by dynamic light scattering (DLS) (Fig. S6, ESI†). Analysis of **ND** indicates a multimodal size distribution (d_H = 98 ± 22, 274 ± 125 and 790 ± 272 nm), which was perhaps expected considering the poor solubility of pristine **ND** in chloroform. DLS measurements of the oxidised nanodiamonds, **ND-COOH**, showed a narrower size distribution, d_H = 301 ± 80 nm. Due to the change in distribution, it was likely that the aggregates in the pristine **ND** sample disassembled during the acid/sonication treatment and then reaggregated in the oxidised sample. These results demonstrated that sonication is enough to break up the pristine **ND** sample and no harsher treatments, such as mixed media milling, are required. For the ND-PDI systems, DLS results showed that the mean aggregate sizes were 873 ± 142 nm (**ND-1a**), 479 ± 188 nm (**ND-1b**) and 219 ± 77 nm (**ND-2**) (Fig. 2f). NDs functionalised with alkane chains or different functional groups have been found in the literature to decrease aggregate size in organic solvents, due to decreased inter-particle interactions.[57] Therefore, a reduction in the size of aggregate for **ND-2** was expected, due to termination of the PDI with aryl groups, but **ND-1a** and **ND-1b** exhibited increased aggregation. This was potentially due to the pendent alcohol groups enhancing inter-particle interactions through hydrogen bonding, as observed in the crystal structure of **1a**. It is also possible that **1a** and **1b**, being bifunctional, could bridge two adjacent nanodiamonds which would also increase the effective aggregate size.

Finally, the effect of tethering the PDIs to NDs was probed by fluorescence spectroscopy. Neither the parent **ND** nor **ND-COOH** exhibit emission under the conditions of the experiment (532 nm excitation). Emission spectra for the parent PDIs, **1a**, **1b** or **2**, both in solution and as powders were collected and compared to spectra collected for powders of their ND-PDI composites (Fig. 3) revealing a common trend. The emission spectra of **ND-1a**, **ND-1b** and **ND-2** showed maxima at 763, 775, and 545/585 nm, respectively. The positions of the emission maxima were all slightly redshifted with respect to the corresponding PDIs in chloroform solution (739, 755 and 540/580 nm, respectively), but a much greater shift was seen with respect to the emission from powder samples of the same PDIs (851, 838 and 645 nm, respectively). Moreover, the emission for **ND-1a**, **ND-1b** and **ND-2**, where PDIs are tethered to NDs, more closely resembles that found for PDIs in solution, as opposed to the solid powder. In the case of **ND-2** even the peak profile of **2** is retained in the ND-PDI composite, but not for the powdered sample of the same compound (Fig. 3c). These spectra confirmed that tethering the PDIs to the nanodiamond support results in the retention of the PDI absorption and emission properties observed for solutions of the parent compounds. Interestingly, mechanical mixtures of nanodiamonds and a further PDI, designated **3** and critically not able to form ester linkages with surface carboxylic acids of **ND-COOH**, did not show the same effect, rather displaying an emission profile akin to the PDI powder (Fig. S7, ESI†). This indicates that PDI molecules, when chemically grafted to the surfaces of NDs, are physically separated from one another such that their optical properties are not perturbed by the intermolecular interactions observed in the crystal form.

Conclusions

We describe a method for tethering strongly absorbing and emitting chromophores, in this case PDIs, to solid nanoscale supports, in this case nanodiamonds. Our simple approach allows the facile synthesis of the ND-PDI composite materials which retain the properties and structure of the nanodiamond supports. A variety of techniques (notably TEM/EDX, DLS and TGA) all suggest that the nanodiamond morphologies and interior cores are unaffected by the functionalisation process. Perhaps most interestingly fluorescence spectroscopy indicates that the properties of the nanodiamond-tethered PDI most closely resemble those of PDI in solution rather than PDI in the solid-state, where a clear red-shift is observed. Thus, the tethering process we describe provides a simple approach to preparing solids with the properties that these fascinating chromophores exhibit in solution. We believe that this approach could be easily developed for other chromophores providing a generic approach to the preparation of materials that maintain the solution-phase behaviour of the target chromophore.

Conflicts of interest

There are no conflicts to declare.

Acknowledgements

The authors are grateful to Dr Olga Levinson (Ray Technologies Ltd.) for providing samples of nanodiamonds and Prof. Andrei Khlobystov for insightful discussions into nanodiamond surface functionalisation and characterisation. ARYA gratefully acknowledges the scholarship and support provided by King Faisal University (Al-Ahsa, Saudi Arabia). NRC gratefully acknowledges the support of the UK Engineering and Physical Sciences Research Council (EP/S002995/1 and EP/N033906/1).

References

1 F. Würthner, *Chem. Commun.*, 2004, 1564–1579.
2 F. Würthner, C. R. Saha-Möller, B. Fimmel, S. Ogi, P. Leowanawat and D. Schmidt, *Chem. Rev.*, 2016, **116**, 962–1052.

3 Z. Chen, U. Baumeister, C. Tschierske and F. Würthner, *Chem. – Eur. J.*, 2007, **13**, 450–465.
4 G. Seybold and G. Wagenblast, *Dyes Pigm.*, 1989, **11**, 303–317.
5 D. Khim, K.-J. Baeg, J. Kim, M. Kang, S.-H. Lee, Z. Chen, A. Facchetti, D.-Y. Kim and Y.-Y. Noh, *ACS Appl. Mater. Interfaces*, 2013, **5**, 10745–10752.
6 M. E. Gemayel, M. Treier, C. Musumeci, C. Li, K. Müllen and P. Samorì, *J. Am. Chem. Soc.*, 2012, **134**, 2429–2433.
7 X. Liu, H. Xu, Y. Zhou, C. Yang, G. Liu, L. Luo, W. Wang, Y. Ma, J. Jin, J. Zhang and W. Huang, *Org. Electron.*, 2020, **83**, 105777.
8 E. Kozma, W. Mróz, F. Villafiorita-Monteleone, F. Galeotti, A. Andicsová-Eckstein, M. Catellania and C. Botta, *RSC Adv.*, 2016, **6**, 61175–61179.
9 G. Li, Y. Zhao, J. Li, J. Cao, J. Zhu, X. W. Sun and Q. Zhang, *J. Org. Chem.*, 2015, **80**, 196–203.
10 F. J. Céspedes-Guirao, S. García-Santamaría, F. Fernández-Lázaro, A. Sastre-Santos and H. J. Bolink, *J. Phys. D: Appl. Phys.*, 2009, **42**, 105106.
11 C. Huang, S. Barlow and S. R. Marder, *J. Org. Chem.*, 2011, **76**, 2386–2407.
12 Z. Liu, Y. Wu, Q. Zhang and X. Gao, *J. Mater. Chem. A*, 2016, **4**, 17604–17622.
13 E. Kozma and M. Catellani, *Dyes Pigm.*, 2013, **98**, 160–179.
14 S. Hüttner, M. Sommer and M. Thelakkat, *Appl. Phys. Lett.*, 2008, **92**, 093302.
15 J. D. Yuen, V. A. Pozdin, A. T. Young, B. L. Turner, I. D. Giles, J. Naciri, S. A. Trammell, P. T. Charles, D. A. Stenger and M. A. Daniele, *Dyes Pigm.*, 2020, **174**, 108014.
16 S. Dey, S. Mahanty, A. Saha, P. Kumar, R. Saha, C. Kar, P. Chaudhuri and P. K. Sukul, *Mater. Adv.*, 2020, **1**, 1817–1828.
17 F. Liu, J. Mu, X. Wu, S. Bhattacharya, E. K. L. Yeow and B. Xing, *Chem. Commun.*, 2014, **50**, 6200–6203.
18 T. E. Kaiser, H. Wang, V. Stepanenko and F. Würthner, *Angew. Chem., Int. Ed.*, 2007, **46**, 5541–5544.
19 R. F. Fink, J. Seibt, V. Engel, M. Renz, M. Kaupp, S. Lochbrunner, H.-M. Zhao, J. Pfister, F. Würthner and B. Engels, *J. Am. Chem. Soc.*, 2008, **130**, 12858–12859.
20 Z. Chen, V. Stepanenko, V. Dehm, P. Prins, L. D. A. Siebbeles, J. Seibt, P. Marquetand, V. Engel and F. Würthner, *Chem. – Eur. J.*, 2007, **13**, 436–449.
21 T. E. Kaiser, H. Wang, V. Stepanenko and F. Würthner, *Angew. Chem., Int. Ed.*, 2007, **46**, 5541–5544.
22 J. Seibt, P. Marquetand, V. Engel, Z. Chen, V. Dehm and F. Würthner, *Chem. Phys.*, 2006, **328**, 354–362.
23 M. Stolte, T. Schembri, J. Süß, D. Schmidt, A.-M. Krause, M. O. Vysotsky and F. Würthner, *Chem. Mater.*, 2020, **32**, 6222–6236.
24 D. Schmidt, M. Stolte, J. Süß, A. Liess, V. Stepanenko and F. Würthner, *Angew. Chem., Int. Ed.*, 2019, **58**, 13385–13389.
25 B. Zhang, P. Zhao, L. J. Wilson, J. Subbiah, H. Yang, P. Mulvaney, D. J. Jones, K. P. Ghiggino and W. W. H. Wong, *ACS Energy Lett.*, 2019, **4**, 1839–1844.
26 R. P. Sabatini, B. Zhang, A. Gupta, J. Leoni, W. W. H. Wong and G. J. Lakhwani, *J. Mater. Chem. C*, 2019, **7**, 2954–2960.
27 B. Zhang, H. Soleimaninejad, D. J. Jones, J. M. White, K. P. Ghiggino, T. A. Smith and W. W. H. Wong, *Chem. Mater.*, 2017, **29**, 8395–8403.
28 J. L. Banal, H. Soleimaninejad, F. M. Jradi, M. Liu, J. M. White, A. W. Blakers, M. W. Cooper, D. J. Jones, K. P. Ghiggino, S. R. Marder, T. A. Smith and W. W. H. Wong, *J. Phys. Chem. C*, 2016, **120**, 12952–12958.
29 X. Cao, S. Bai, Y. Wu, Q. Liao, Q. Shi, H. Fu and J. Yao, *Chem. Commun.*, 2012, **48**, 6402–6404.
30 M.-J. Lin, A. J. Jiménes, C. Burschka and F. Würthner, *Chem. Commun.*, 2012, **48**, 12050–12052.
31 Á. J. Jiménes, M.-J. Lin, C. Burschka, J. Becker, V. Settels, B. Engels and F. Würthner, *Chem. Sci.*, 2014, **5**, 608–619.
32 S. Nakazono, Y. Imazaki, H. Yoo, J. Yang, T. Sasamori, N. Tokitoh, T. Cédric, H. Kageyama, D. Kim, H. Shinokubo and A. Osuka, *Chem. – Eur. J.*, 2009, **15**, 7530–7533.
33 H. Langhals, O. Krotz, K. Polborn and P. Mayer, *Angew. Chem., Int. Ed.*, 2005, **44**, 2427–2428.
34 G. Seybold and G. Wagenblast, *Dyes Pigm.*, 1989, **11**, 303–317.
35 O. A. Shenderova, V. V. Zhirnov and D. W. Brenner, *Crit. Rev. Solid State Mater. Sci.*, 2002, **27**, 227–356.
36 A. M. Schrand, S. A. C. Hens and O. A. Shenderova, *Crit. Rev. Solid State Mater. Sci.*, 2009, **34**, 18–74.
37 A. M. Schrand, S. A. C. Hens, O. A. Shenderova, V. V. Zhirnov, D. W. Brenner, R. Kaur and I. Badea, *Crit. Rev. Solid State Mater. Sci.*, 2013, **34**, 18–74.
38 N. R. Greiner, D. S. Phillips, J. D. Johnson and F. Volk, *Nature*, 1988, **333**, 440–442.
39 Y. Zhang, K. Y. Rhee, D. Hui and S.-J. Park, *Composites, Part B*, 2018, **143**, 19–27.
40 C.-C. Fu, H.-Y. Lee, K. Chen, T.-S. Lim, H.-Y. Wu, P.-K. Lin, P.-K. Wei, P.-H. Tsao, H.-C. Chang and W. Fann, *Proc. Natl. Acad. Sci. U. S. A.*, 2007, **104**, 727–732.
41 H. Huang, E. Pierstorff, E. Osawa and D. Ho, *Nano Lett.*, 2007, **7**, 3305–3314.
42 I. S. P. Michail, D. Ivanov, I. Petrov, G. McGuire and O. Shenderova, *MRS Proceedings*, 2009, **1203**, 1203.
43 J. T. Paci, H. B. Man, B. Saha, D. Ho and G. C. Schatz, *J. Phys. Chem. C*, 2013, **117**(33), 17256–17267.
44 S. Mallakpour and S. Soltanian, *RSC Adv.*, 2016, **6**, 109916–109935.
45 K. D. Behler, A. Stravato, V. Mochalin, G. Korneva, G. Yushin and Y. Gogotsi, *ACS Nano*, 2009, **3**, 363–369.
46 D. H. Wang, L.-S. Tan, H. Huang, L. Dai and E. Osawa, *Macromolecules*, 2009, **42**, 114–124.
47 J. Cheng, J. He, C. Li and Y. Yang, *Chem. Mater.*, 2008, **20**, 4224–4230.
48 V. N. Mochalin, I. Neitzel, B. J. M. Etzold, A. Peterson, G. Palmese and Y. Gogotsi, *ACS Nano*, 2011, **5**, 7494–7502.
49 G. Goretzki, E. S. Davies, S. P. Argent, W. Alsindi, A. J. Blake, J. E. Warren, J. McMaster and N. R. Champness, *J. Org. Chem.*, 2008, **73**, 8808–8814.

50 B. A. Llewellyn, E. S. Davies, C. R. Pfeiffer, M. Cooper, W. Lewis and N. R. Champness, *Chem. Commun.*, 2016, **52**, 2099–2102.
51 S. L. Haddow, D. J. Ring, H. Bagha, H. Nowell, N. Pearce, H. Nowell, A. J. Blake, W. Lewis, J. McMaster and N. R. Champness, *Cryst. Growth Des.*, 2018, **18**, 802–807.
52 M. Franceschin, A. Alvino, V. Casagrande, C. Mauriello, E. Pascucci, M. Savino, G. Ortaggi and A. Bianco, *Bioorg. Med. Chem.*, 2007, **15**, 1848–1858.
53 N. Pearce, E. S. Davies, W. Lewis and N. R. Champness, *ACS Omega*, 2018, **3**, 14236–14244.
54 C.-L. Park, A. Y. Jee, M. Le and S. Lee, *Chem. Commun.*, 2009, 5576–5578.
55 C.-L. Park, A. Young Jee, M. Lee and S. Lee, *Chem. Commun.*, 2009, 5576–5578.
56 T. Petit and L. Puskar, *Diamond Relat. Mater.*, 2018, **89**, 52–66.
57 A. Krueger and T. Boedeker, *Diamond Relat. Mater.*, 2008, **17**, 1367–1370.